

U.S. DEPARTMENT OF COMMERCE  
National Technical Information Service

AD-A032 287

WAVEGUIDE-MODE POWER BUDGET FOR AN ELF/VLF  
TRANSMITTING SATELLITE

NAVAL RESEARCH LABORATORY, WASHINGTON, D. C.

SEPTEMBER 17, 1976

329133

NRL Report 8032

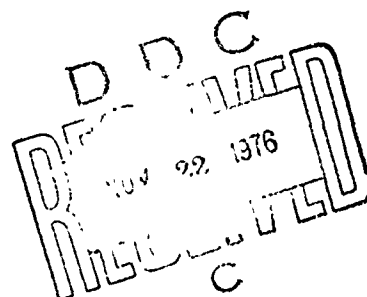
# Waveguide-Mode Power Budget for an ELF/VLF Transmitting Satellite

F. J. KELLY, G. A. CHAYT, AND D. J. BAKER

*Electromagnetic Propagation Branch  
Communications Sciences Division*

AD A032287

September 17, 1976



REPRODUCED BY  
NATIONAL TECHNICAL  
INFORMATION SERVICE  
U. S. DEPARTMENT OF COMMERCE  
SPRINGFIELD, VA. 22161

NAVAL RESEARCH LABORATORY  
Washington, D.C.

Approved for public release; distribution unlimited.

SECURITY CLASSIFICATION OF THIS PAGE (When Data Entered)

REPORT DOCUMENTATION PAGE		READ INSTRUCTIONS BEFORE COMPLETING FORM
1. REPORT NUMBER NRL Report 8032	2. GOVT ACCESSION NO.	3. RECIPIENT'S CATALOG NUMBER
4. TITLE (and Subtitle) WAVEGUIDE-MODE POWER BUDGET FOR AN ELF/VLF TRANSMITTING SATELLITE		5. TYPE OF REPORT & PERIOD COVERED A final report on one phase of a continuing NRL problem.
		6. PERFORMING ORG. REPORT NUMBER
7. AUTHOR(s) F. J. Kelly, G. A. Chayt, and D. J. Baker		8. CONTRACT OR GRANT NUMBER(s)
9. PERFORMING ORGANIZATION NAME AND ADDRESS Naval Research Laboratory Washington, D.C. 20375		10. PROGRAM ELEMENT, PROJECT, TASK AREA & WORK UNIT NUMBERS NRL Problem R07-30 RF21-222-402 NASA W14.148
11. CONTROLLING OFFICE NAME AND ADDRESS Department of the Navy Office of Naval Research Arlington, Virginia 22217		12. REPORT DATE September 17, 1976
		13. NUMBER OF PAGES 25
14. MONITORING AGENCY NAME & ADDRESS (if different from Controlling Office)		15. SECURITY CLASS. (of this report) Unclassified
		15a. DECLASSIFICATION/DOWNGRADING SCHEDULE
16. DISTRIBUTION STATEMENT (of this Report)  Approved for public release; distribution unlimited.		
17. DISTRIBUTION STATEMENT (of the abstract entered in Block 20, if different from Report)		
18. SUPPLEMENTARY NOTES		
19. KEY WORDS (Continue on reverse side if necessary and identify by block number) Antenna radiation patterns      Transionospheric propagation Extremely low frequency (ELF)      Very low frequency (VLF) Satellite      Waveguide mode propagation		
20. ABSTRACT (Continue on reverse side if necessary and identify by block number) Signal-to-noise (S/N) ratio power budgets are evaluated for an ELF/VLF transmitting satellite using waveguide-mode field representations in the frequency range from 250 Hz to 9 kHz and for satellite heights from 120 km to 800 km. The low-order waveguide-mode parameters are presented. The propagation of the waveguide-mode fields into the lower ionosphere is evaluated using a full wave method. The propagation of the fields in the upper ionosphere is evaluated by a ray-tracing method. When these fields are known, the propagation from a ground-based transmitter to a satellite receiver may be evaluated, as well as the reciprocal transmission from a satellite transmitter to (Continued)		

DD FORM 1473

EDITION OF 1 NOV 65 IS OBSOLETE  
S/N 0102-014-6101

SECURITY CLASSIFICATION OF THIS PAGE (When Data Entered)

a ground-based receiver. The radiation resistance of a finite loop magnetic dipole antenna is evaluated for a variety of frequencies and locations in the ionosphere for both open and closed index of refraction surfaces.

The satellite power required to provide a S/N ratio in excess of 0 dB in a 1-Hz bandwidth at a 1-Hertz bandwidth at a ground range of 1 Mm from the ionospheric exit point of the waves is evaluated for several cases. The power requirements (in the megawatt range) exceed the power supplied on current spacecraft missions, but they are within the realm considered possible for future space electric power systems.

## CONTENTS

	Page
INTRODUCTION .....	1
THEORY .....	2
CALCULATIONS AND RESULTS .....	9
DISCUSSION .....	19
ACKNOWLEDGMENTS .....	20
REFERENCES .....	20

ACCESSION FOR \_\_\_\_\_

NTIS \_\_\_\_\_

U. S. \_\_\_\_\_

COVER SHEET \_\_\_\_\_

DESCRIPTION \_\_\_\_\_

BY \_\_\_\_\_

CONTRIBUTOR, AVAILABLE \_\_\_\_\_

DATE \_\_\_\_\_

A

## WAVEGUIDE-MODE POWER BUDGET FOR AN ELF/VLF TRANSMITTING SATELLITE

### INTRODUCTION

The study of electromagnetic propagation from a satellite to ground at extremely low frequencies (ELF) or very low frequencies (VLF) is an interesting and important problem since LF electromagnetic waves can penetrate to significant depths below the earth's surface for reception at submerged or buried antennas. These waves have unusual characteristics because the ionospheric plasma and the earth's magnetic field govern the directions in which the waves are generated and propagated. The waves exhibit a strong tendency to follow the direction of the earth's magnetic field while they are within the ionosphere (Fig. 1). When they emerge below the ionosphere, they enter a leaky waveguide formed between the edge of the lower ionosphere and the earth's surface, and propagate via waveguide modes to be received at distant points on the earth's surface. In the literature this waveguide is often referred to as the earth-ionosphere waveguide.

Numerous calculations and experiments have been performed concerning the propagation of ELF and VLF electromagnetic waves from point to point within the waveguide. Galejs [1,2], Einaudi and Wait [3,4] and Pappert [5] have previously treated the problem of the excitation of waveguide modes by transmitting electric or magnetic dipoles at satellite heights. While these treatments specified the magnetic or electric dipole moment required at the satellite to achieve a given field at some distant point on the earth's surface, they did not further specify the electrical powers that are required to produce the electric or magnetic dipole moment in a given realizable antenna. The present report adds this important information to the problem for the transmitting magnetic dipole antenna. Calculations of radiation resistance are performed for various transmitting antenna sizes and heights at several frequencies using the methods described by Baker [6]. The ohmic resistance of a loop is readily calculable from the loop antenna size parameters knowing the conductivity of the loop material. In this report the loop antenna is considered to be made of aluminum and to operate at room temperature.

The transmitter power required to produce a given signal-to-noise ratio (S/N) at a given point on the earth's surface is strongly dependent on the exact circumstances under which the communications circuit is needed. For example, the required power depends on the satellite antenna size, altitude and composition, the transmission frequency, the required S/N ratio for communications, the time of day, season of the year and the size and geographical location of the desired coverage area. The first results presented in this paper are applicable to a winter nighttime propagation model, which is probably the most favorable condition for the operation of a communication circuit. We then consider the increased requirement presented by the summer nighttime noise, and finally the further increased requirement caused by lossy daytime transionospheric propagation during both the winter and summer.

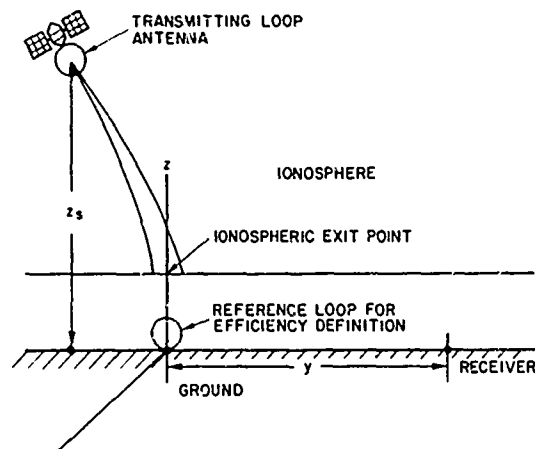


Fig. 1—Illustration of propagation path from ELF/VLF transmitting satellite to the ionospheric exit point. The Cartesian coordinate frame for the calculation of field components is shown

## THEORY

The excitation of waveguide modes by a satellite-borne transmitter has been considered previously. Galejs [1,2] gave the first treatment of the efficiency by which an antenna in the ionosphere can excite a mode in the earth-ionosphere waveguide. He showed that the relative efficiency of a transmitting antenna in the ionosphere is at most approximately equal to that of an optimally located antenna in the earth-ionosphere waveguide, and it is usually much less efficient. His numerical results are for frequencies between 10 and 1000 Hz and between 10 kHz and 30 kHz daytime and nighttime propagation conditions. Einaudi and Wait [3,4] give some numerical results for a normalized excitation factor of the zero order waveguide mode in the frequency range between 500 Hz and 7.0 kHz for the case of a vertical antenna and a vertical magnetic field. The values of the relative excitation factor are much smaller than those predicted for an equivalent transmitting dipole moment optimally oriented within the earth-ionosphere waveguide. However, Einaudi and Wait assume free space propagation both below and above the plasma slab representing the D-region.

Pappert [5] has calculated the excitation of the earth-ionosphere waveguide at extremely low frequencies for a satellite at 9500-km height using a realistic nighttime ionosphere profile and several geomagnetic dip angles and propagation directions. His results indicate that at 75 Hz, a horizontal electric dipole in the ionosphere would be approximately 5 dB more efficient than a similar horizontal dipole laid on a poorly conducting ( $\sigma \approx 10^{-4}$  mho/m) earth (similar to the proposed SANGUINE/SEAFARER antenna). However, Pappert states that an "excessively large" magnetic dipole moment would be required to give long-range communications coverage similar to a SANGUINE/SEAFARER transmitting system.

A waveguide-mode power budget at a given frequency requires that the mode propagation parameters be known. Barr [7-11], Galejs [12], and Wait [13] have given numerical values of the waveguide-mode propagation parameters in the frequency range of interest. Barr has given especially complete results in the 1-10 kHz range for numerous daytime ionosphere electron density profiles. Computer programs [14] are available for calculating waveguide-mode propagation parameters for arbitrary electron and ion density profiles, geomagnetic dip angles, and propagation direction.

The computer program of Pappert, et al. [14] determines the waveguide-mode parameters by finding the roots of an equation involving the ionosphere and ground reflection coefficients. It does not give values of the fields within the ionosphere, so an alternative approach, such as that of Pitteway [15], must be used to determine the structure of the waveguide-mode fields within the ionosphere.

In the present study, waveguide-mode calculations are performed in the frequency range from 250 Hz to 9 kHz. Calculations are made of the required magnetic moment which a satellite must produce to provide a usable S/N ratio at one megameter (Mm) from the ionospheric exit point. The power needed to generate this magnetic moment using a loop antenna is calculated using the methods of Baker, et al. [6]. Although some effort is made here to optimize the selection of satellite height, frequency of operation, and loop antenna radius, it is not possible to optimize the system fully due to funding constraints. A selection of alternate frequencies or a different loop antenna radius might reduce the calculated powers significantly.

Figure 1 shows a Cartesian coordinate system in which the vertical coordinate of the transmitter's location is denoted by  $z_s$ . The distance between the point on the earth's surface beneath the ionospheric exit point and the receiver is  $y$ . The  $x$  axis in this coordinate system is perpendicular to the direction of wave propagation. An arbitrary dipping static magnetic field can be inserted in this system, such that it will maintain a constant angle with respect to the direction of propagation of the wave. The resultant Maxwell's equations can be factored into  $z$  and  $y$ -dependent terms and solved by a separation of variables technique.

The relative efficiency  $\eta_{ij}^{(n)}(z_s)$  of a magnetic dipole transmitter, located at some height  $z_s$  in the ionosphere, for exciting the  $n$ th mode of the earth-ionosphere waveguide may be defined as the ratio of a waveguide-mode field produced by a satellite transmitting antenna to the waveguide-mode field produced by an equivalent transmitting antenna situated on the earth's surface. In this definition, the transmitting antenna on the earth's surface must have the same magnetic dipole moment as the satellite-borne antenna, and be located at a point on the earth's surface exactly below the ionospheric exit point of the waves transmitted by the satellite. The waveguide-mode fields generated by the two antennas must be produced at the earth's surface at the same distance and direction from the ionospheric exit point. The orientations of the satellite dipole and the dipole on the earth's surface must be specified to complete this definition. Thus, the relative efficiency  $\eta_{iz}^{(n)}(z_s)$  of a vertical magnetic dipole at height  $z_s$  in the ionosphere for exciting a given waveguide mode may be defined as the ratio of the  $z$ -component of the electric field in the  $n$ th waveguide mode produced at the earth's surface by this satellite transmitting antenna to the same field component produced by an equivalent antenna on the earth's surface. In this definition, the transmitting antenna on the earth's surface must have the same vertical magnetic dipole moment as the satellite-borne antenna, and be located at a



point on the earth's surface exactly below the ionospheric exit point of the waves transmitted by the satellite. The waveguide-mode fields in the  $n$ th waveguide mode must be produced at the earth's surface at the same distance and direction from the ionospheric exit point. The relative efficiency of a horizontal magnetic dipole transmitter in the ionosphere can be defined in the same way; however, the reference ground-based transmitting dipole could be either horizontal or vertical, and, if horizontal, it could be oriented either parallel, perpendicular, or at some arbitrary angle to the direction of propagation of the waveguide mode. Because of the flexibility of the choice of the reference dipole's orientation, there are at least nine possible efficiency definition combinations for magnetic dipole transmitters, and nine more for electric dipole transmitters. We will restrict our attention in this paper to magnetic dipole antennas, and will select a reference antenna with the best orientation for exciting the mode in question.

Galejs [1] and Pappert [5] show that the efficiency ratio as discussed above is equal to the ratio of the respective field component values of the waveguide mode propagating in the opposite direction (from the receiver toward the source), where the numerator of the ratio is the field component evaluated in the ionosphere, the denominator is the field component evaluated at the earth's surface, and the direction of the earth's magnetic field is inverted. Thus, the relative efficiency of a vertical electric dipole in the ionosphere to one on the earth's surface for exciting a given waveguide mode is numerically equal to the ratio of the vertical electric field present in that waveguide mode at that height in the ionosphere to the vertical electric field carried by that waveguide mode at a point on the earth's surface directly below the ionospheric exit point (when the direction of propagation of the mode and the direction of the earth's magnetic field have been inverted).

The vertical electric field  $E_z(0, y)$  generated at the surface of the earth by a transmitting satellite loop antenna at a height  $z_s$ , having current  $I$  and area  $da$ , can be calculated from the following:

$$\frac{E_z(0, y)[by Ida(z_s)|_j]}{E_z(0, y)[by Ida(0)|_i]} = \frac{H_j(z_s)Ida(z_s)|_j}{H_i(0)Ida(0)|_i} \quad (1)$$

where

$E_z(0, y)[by Ida(z_s)|_j]$  is the vertical electric field at the earth's surface generated by a source having magnetic dipole moment  $Ida(z_s)$  at the height  $z_s$ , oriented with the dipole moment along the  $j$ th axis,

$E_z(0, y)[by Ida(0)|_i]$  is the vertical electric field at the earth's surface generated by a source having magnetic dipole moment  $Ida(0)$  at the earth's surface, oriented with the dipole moment along the  $i$ th axis,

$H_j(z_s)$  is the  $j$ th component of the magnetic field at height  $z_s$ ,

$H_i(0)$  is the  $i$ th component of the magnetic field at the surface of the earth,

NRL REPORT 8032

$Ida(z_s)|_j$  is the magnetic dipole moment of a loop transmitter located at height  $z_s$ , oriented with the dipole moment along the  $j$ th axis,

$I$  is the current in the loop,

$da(z_s)$  is the area of the loop,

Setting

$$Ida(z_s)|_j = Ida(0)|_i \quad (2)$$

we obtain

$$\eta_{ij}(z_s) = \frac{E_z(0,y)[by Ida(z_s)|_j]}{E_z(0,y)[by Ida(0)|_i]} = \frac{H_j(z_s)}{H_i(0)} \quad (3)$$

The coordinates  $i$  and  $j$  can be arbitrarily chosen in (1-3). In this report we will concentrate on the TM-mode fields, because they are most effective for communications to receivers located at or below the earth's surface. A magnetic loop transmitter will be considered because the power losses of such a transmitter are readily calculable [6]. The reference magnetic loop transmitting antenna is located on the earth's surface with its axis parallel to the  $x$  axis (Fig. 1). This is the optimum orientation for generating a TM-mode wave propagating in the  $y$  direction, and is most meaningful in referring the TM-mode fields from a satellite transmitter to the fields produced by a loop antenna at the earth's surface. The efficiency of a satellite transmitter is then given by

$$\eta_{xj}(z_s) = \frac{H_j(z_s)}{H_x(0)} \quad (4)$$

Equations for the fields at a point at distance  $y$  from a loop transmitter in the earth-ionosphere waveguide have been given by Galejs [12] for all components of the  $E$  and  $H$  fields. The equations for the contributions by the TM-mode fields to the vertical electric and horizontal magnetic fields are

$$E_z(z,y) = \omega \eta_0 Ida \sum_n S_n^{0.5} F_n \quad (5)$$

$$H_x(z,y) = -k_0 Ida \sum_n S_n^{-0.5} F_n \quad (6)$$

where

$$F_n = \frac{1}{h\sqrt{y\lambda}} \sqrt{\frac{y/a}{\sin(y/a)}} G_n(z) G_n(z_s) \Lambda_n \exp(i\pi/4 + ik_0 y S_n) \quad (7)$$

$a$  = the radius of the earth (m),

$z$  = the receiver height (m),

$z_s$  = the transmitter height (m),

$\Lambda_n$  = the excitation factor of the  $n$ th mode,

$S_n$  = the sine of the eigenangle of the  $n$ th waveguide mode,

$y$  = the great circle distance between the wave exit point and receiver (m),

$\lambda$  = the free-space wavelength of the wave (m),

$k_0 = 2\pi/\lambda$  ( $\text{m}^{-1}$ ),

$I$  = current of loop (amps),

$G_n$  = the height gain function of the  $n$ th mode,

$da$  = area of loop ( $\text{m}^2$ ),

$\omega$  = angular frequency of wave =  $2\pi f$  Hz,

$\mu_0$  = permeability of free space =  $4\pi \times 10^{-7}$ ,

$h$  = the height of the waveguide (m).

Equations (5-7) apply to the case in which both the transmitter and receiver are within the waveguide ( $0 < z, z_s < h$ ). The sine of the mode eigenangle  $S_n$  is related to the attenuation rate  $\alpha$  and the phase velocity  $v_{ph}$  of the waveguide-mode waves according to Galejs [14]:

$$\text{Re}(S_n) = c/v_p \quad (8)$$

$$\alpha = 0.02895 \omega \text{Im}(S_n) \text{ (in dB/Mm)}. \quad (9)$$

In (8),  $c$  is the speed of light.

The following procedure is used to calculate  $\eta_{ij}(z_s)$ . First, the mode eigenangle and the values of the electric field components at several heights in the waveguide are calculated according to the method of Pappert, et al. [14]. Based on the eigenangle of an incident wave on the lower ionosphere, the wavefield of the penetrating and nonpenetrating

waves are calculated at the same heights in the waveguide and at selected heights in the ionosphere according to the procedure of [15-17].

Next, the coefficients  $b_n$  and  $b_p$  are determined applying Cramer's Rule to (10-12). In this way, the waveguide mode may be constructed from a linear combination of the penetrating and nonpenetrating field solutions:

$$E_z^{(n)}(z) = b_p E_z^{pen}(z) + b_n E_z^{non}(z) \quad (10)$$

$$E_y^{(n)}(z) = b_p E_y^{pen}(z) + b_n E_y^{non}(z) \quad (11)$$

$$E_x^{(n)}(z) = b_p E_x^{pen}(z) + b_n E_x^{non}(z). \quad (12)$$

In the above equations,

$E_x^{(n)}(z)$ ,  $E_y^{(n)}(z)$ , and  $E_z^{(n)}(z)$  are the components of the  $n$ th waveguide-mode electric vector at height  $z$  in the waveguide,

$E_x^{pen}(z)$ ,  $E_y^{pen}(z)$ , and  $E_z^{pen}(z)$  are the components of the electric vector of the penetrating wave at the height  $z$ ,

$E_x^{non}(z)$ ,  $E_y^{non}(z)$ , and  $E_z^{non}(z)$  are the components of the electric vector of the nonpenetrating wave at the height  $z$ .

Coefficients  $b_p$  and  $b_n$  giving the contributions of the penetrating and nonpenetrating waves in forming a waveguide mode. Any pair of (10-12) constitute two equations in two unknowns ( $b_p$ ,  $b_n$ ), and permit the values of  $b_p$  and  $b_n$  to be readily determined by applying Cramer's Rule. The consistency of the values of the third equation may be used as an independent check. In addition, similar sets of field values may be obtained at other heights in the waveguide and additional sets of equations used to check the accuracy of  $b_n$  and  $b_p$ . The waveguide-mode fields in the ionosphere may be readily determined from the  $b_n$  and  $b_p$  amplitudes and the values of the penetrating and nonpenetrating wavefields in the ionosphere. The efficiency  $\eta_{xj}^{(n)}(z_s)$  for the  $n$ th-order TM mode is given by

$$\eta_{xj}^{(n)}(z_s) = \frac{b_p H_j^{pen}(z_s) + b_n H_j^{non}(z_s)}{b_p H_x^{pen}(0) + b_n H_x^{non}(0)} \quad (13)$$

where  $H_j^{pen}(z_s)$  and  $H_j^{non}(z_s)$  are the magnetic fields of the penetrating and nonpenetrating waves at height  $z_s$ .

To determine the waveguide-mode fields at some distance  $y$  from the ionospheric exit point, we multiplied the terms in the mode summations of the right-hand side of (5-6) by the efficiency value  $\eta_{xj}(z_s)$  of the appropriate mode for the appropriate satellite loop orientation and height. The transmitter height gain function  $G_n(z_s)$  which enters in the calculation of  $F_n$  is replaced by the function  $\eta_{xj}^{(n)}(z_s)$ . The results are

$$F_n = \frac{1}{h\sqrt{y\lambda}} \sqrt{\frac{y/a}{\sin(y/a)}} G_n(z) \eta_{xj}^{(n)}(z_s) \Lambda_n \exp(i\pi/4 + ik_0 y S). \quad (14)$$

The approximation of geometric optics may be applied to obtain an approximation to the wave guide-mode fields at considerable heights above the lower  $D$  and  $E$ -ionospheric region. The equations of Ginzburg [18] may be expressed as

$$E_{x,y}(z) = (E_{x,y})_0 (n_0 |n(z)|)^{1/2} \exp \left[ iw \left( t - c^{-1} \int_{z_0}^z n(z) dz \right) \right] \quad (15)$$

$$H_{x,y}(z) = (H_{x,y})_0 (n(z) |n_0|)^{1/2} \exp \left[ iw \left( t - c^{-1} \int_{z_0}^z n(z) dz \right) \right] \quad (16)$$

$(E_{x,y})_0$  and  $(H_{x,y})_0$  are electric and magnetic fields at height  $z_0$ ,

$E_{x,y}(z)$  and  $H_{x,y}(z)$  are electric and magnetic fields at height  $z$ ,

$n_0$  and  $n(z)$  are the indices of refraction of the propagating wave at heights  $z_0$  and  $z$ , respectively.

Thus, the magnetic field achieves a maximum value where the index of refraction is maximum. The value of the  $\eta_j^{(n)}(z_s)$  efficiency ratio may be written

$$\eta_{xj}^{(n)}(z_s) = \eta_{xj}^{(n)}(120km) [\eta(z_s) |\eta(120km)|]^{1/2} \quad (17)$$

$$[ \times \exp[iw(t - c^{-1} \int_{z_0}^z \eta(z) dz)]$$

in terms of the efficiency at 120 km, the indices of refraction at  $z_0$  (120 km), and the transmitter height  $z_s$ .

The input power to the antenna required to produce a 0-dB S/N ratio in a 1-Hz bandwidth is given by

$$P_{\text{req}} = I_{\text{req}}^2 (R_{\text{ohm}} + R_{\text{rad}}) \quad (18)$$

where

$R_{\text{ohm}}$  is the ohmic resistance of the loop,

$R_{\text{rad}}$  is the radiation resistance of the loop,

$$I_{\text{req}} = N(f) [-k_0 da \sum_n S_n^{-0.5} F_n]^{-1}, \quad (19)$$

# NRL REPORT 8032

$N(f)$  = the rms effective magnetic field noise in a 1-Hz bandwidth,

$dA$  = the area of the loop antenna.

In the above equation,  $\eta_{ij}^{(n)}(z_s)$  is given by (13) between 68 and 120 km, and by (17) for transmitter heights above 120 km.

## CALCULATIONS AND RESULTS

For nighttime propagation conditions the Deeks winter nighttime ionosphere electron density profile, as given by Galejs [12], was used (Fig. 2) with the value of collision frequency as given below:

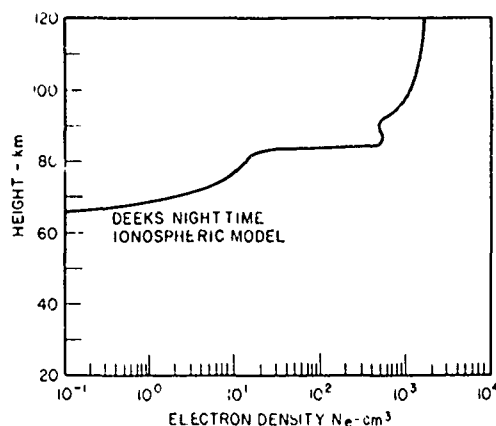


Fig. 2—Ionospheric electron density profile (From Fig. 22, Terrestrial Propagation of Long Electromagnetic Waves, by J. Galejs, Pergamon Press, Copyright 1972 by J. Galejs; used by permission.)

$$\nu_e(z) = 1.8158 \times 10^{11} \exp(-15z). \quad (20)$$

Figures 3, 4, and 5 show propagation parameters as a function of frequency for the Deeks winter nighttime electron density profile. Results are given for three different waveguide modes that propagate readily between 0.5 and 10.0 kHz. The direction of propagation for this mode was due north and the dip angle was 60°.

Figures 6 and 7 show the height variation of the efficiency ratio for Quasi-TE and Quasi-TM mode fields at 6 kHz. Figure 8 shows the efficiency variation for the zero order mode at 250 Hz.

Figures 9 and 10 give the efficiency ratio for 9-kHz Quasi-TM and Quasi-TE modes. In calculating the results of Figs. 3-10, the ionospheric electron density parameters between 100 and 120 km were held constant, equal to the density at 100 km.

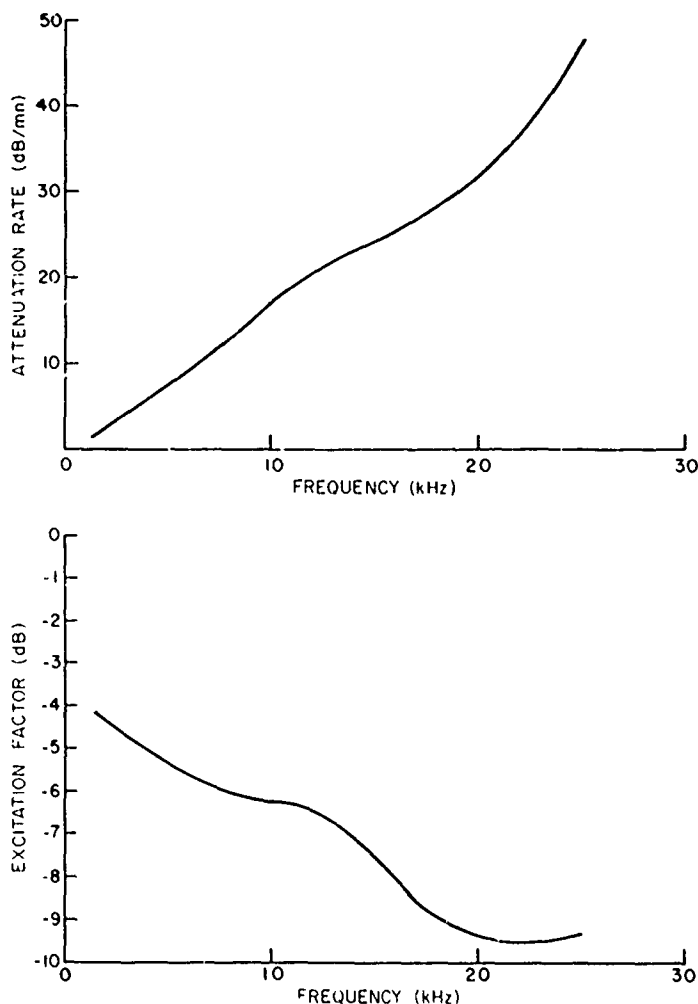


Fig. 3—Lowest-order TEM mode propagation parameters vs frequency

To determine  $\eta_{xj}^{(i)}(z_s)$  for heights between 100 and 1000 km, a ray trace was performed using the procedures and ionosphere model A-3 (for a winter nighttime ionosphere) described by Kelly, et al. [19]. Figure 11 shows curves of  $n(z)$  for frequencies between 250 Hz and 10 kHz.

The net radiation resistance of a loop antenna having a radius of 100 m was calculated according to procedures given by Baker, et al. [6] as a function of ionospheric height at frequencies between 250 Hz and 10 kHz, and is displayed in Fig. 12. Results are given for the loop oriented parallel or perpendicular to the magnetic field. Ohmic resistances of loop antennas are readily calculated. For cases in which the ohmic loss is much greater than the radiated power, it is usually possible to improve the ratio of radiated power to ohmic power by increasing the loop radius. At 250 Hz and 1 kHz, we used the zero-order TEM-mode parameters. At 6000 and 9000 kHz, we used the modal parameters of the first-order TM mode. Additional modes would certainly contribute to

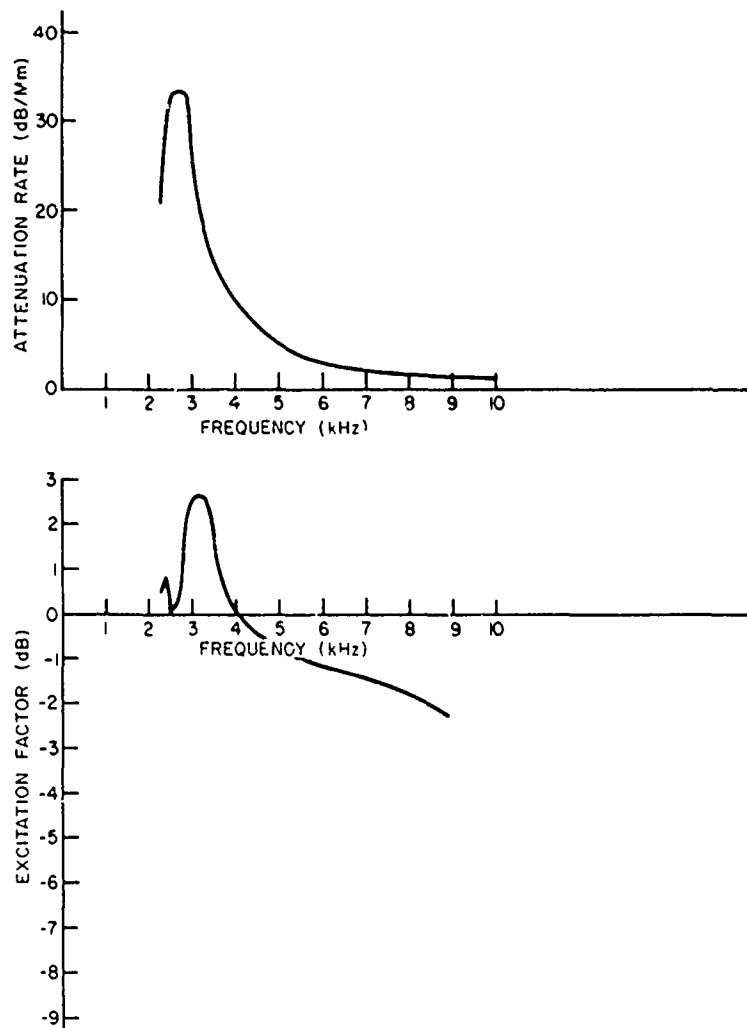


Fig. 4—First-order TM mode propagation parameters vs frequency

the fields at the earth's surface at 1000 km from the subsatellite point, but the dominant contribution would normally be provided by these two low-order modes.

Tables 1 through 4 present the required satellite transmitter powers for several transmitter frequencies, and altitudes for various noise and propagation conditions. In these tables the radiated power, ohmic loss power, and total power are denoted by  $P_{rad}$ ,  $P_{ohmic}$ , and  $P_{total}$ , respectively. Table 1 gives the results calculated for winter nighttime noise and propagation conditions. Tables 2, 3, and 4 contain the results for summer day and night and for winter day conditions, and are simply an extrapolation of the winter nighttime results by the application of appropriate propagation loss and atmospheric noise differences. This simplification of the calculations is justified in light of the uncertainties and variabilities of the ionospheric models. Thus, Table 2 was generated for summer nighttime conditions by using the same propagation calculations as in Table 1,



KELLY, CHAYT AND BAKER

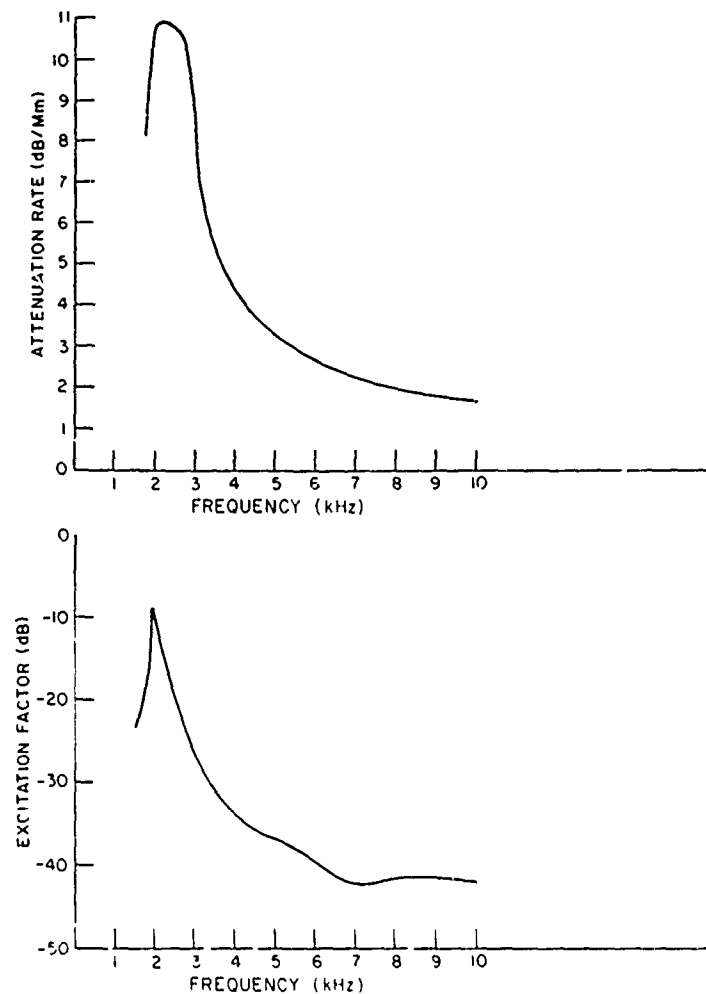


Fig. 5—First-order TE mode propagation parameters vs frequency

and by increasing the atmospheric noise level as predicted by Watt [20] for the summer nighttime Mediterranean Sea area. The values of the daytime and nighttime atmospheric noise at 250 Hz in the Mediterranean Sea are taken as -140 dB below 1 amp/m during summer and -146 dB below 1 amp/m during the winter period. These values are characteristic of 75-Hz measured values [21] and are probably higher than expected at 250 Hz.

At 6 kHz the efficiency factor  $\eta_{xx}$  (120) is approximately 6 dB lower for a wave propagating south from the ionospheric exit point than for a wave propagating north. At 250 Hz and 1 kHz the efficiencies for exciting the north and south propagating waves differ by less than 2 dB. The calculated results in Tables 1 through 4 are valid for the case in which the wave propagates north from the ionospheric exit point.

The predictions of Tables 3 and 4 for summer and winter daytime conditions were obtained using Watt's [20] noise values for the appropriate times and by increasing the transionospheric propagation loss by the amounts derived from Table 5. The nighttime attenuations shown in Table 5 were deduced by averaging separately the daytime and

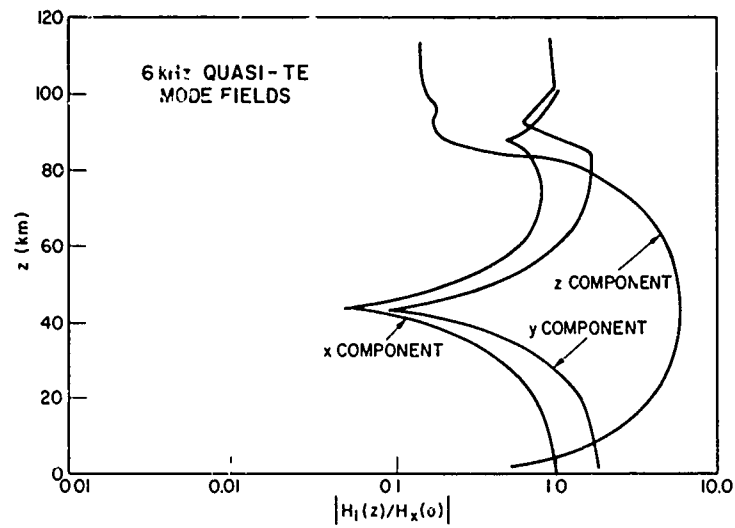


Fig. 6—Relative excitation efficiency vs height of the first-order TE mode at 6.0 kHz

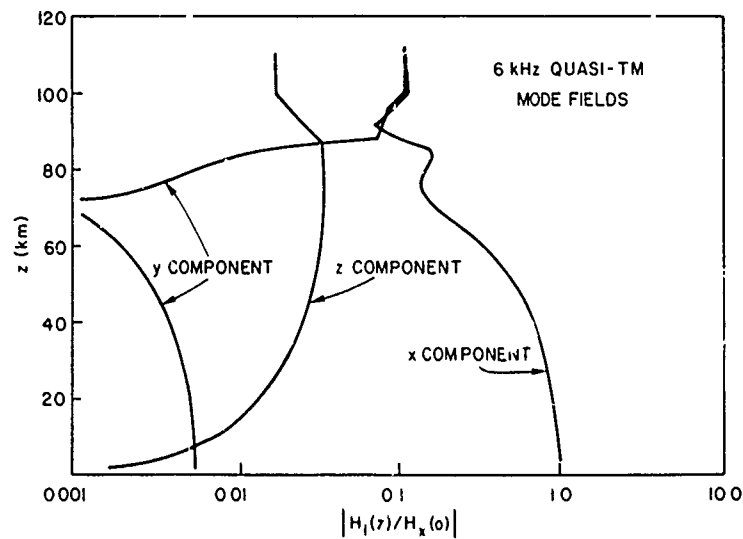


Fig. 7—Relative excitation efficiency v. height of the first-order TM mode at 6.0 kHz

nighttime loss values predicted by the calculations of Pitteway and Jespersen [15], Booker, Crain, and Field [22], Al'pert and Fligel [23], and Helliwell [24]. The daytime power requirements were also increased by an additional factor because of the extra attenuation that the waves undergo in propagating from the ionospheric exit point to the receiver location at 1 Mm range. The calculations of Barr [7] for six different ionospheric models were averaged to determine a mean daytime attenuation rate for the TEM and TM modes used in the present calculations. The average attenuation rates are given in Table 6.

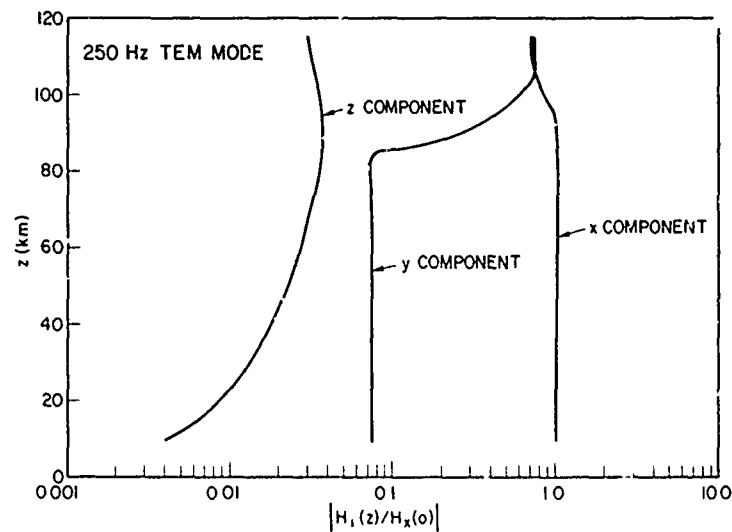


Fig. 8—Relative excitation efficiencies vs height of the zero-order TEM mode at 0.25 kHz

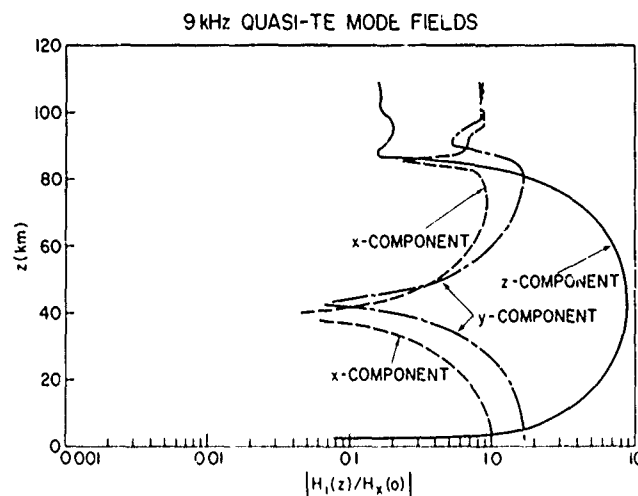


Fig. 9 Relative excitation efficiency vs height of the first order TE mode at 9.0 kHz

NRL REPORT 8032

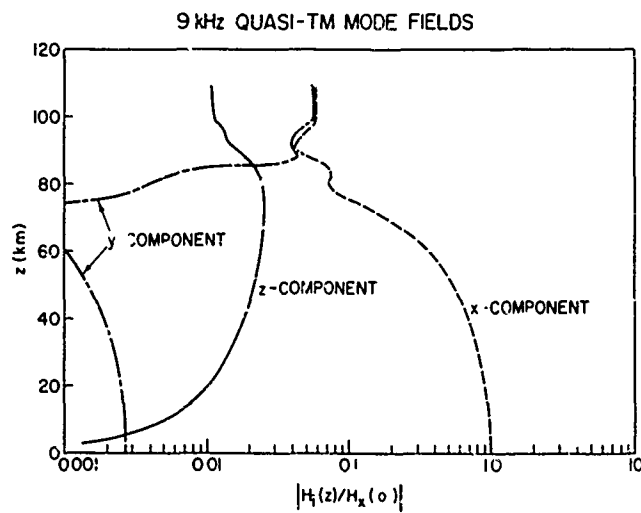


Fig. 10—Relative excitation efficiency vs height of the first-order TM mode at 9.0 kHz

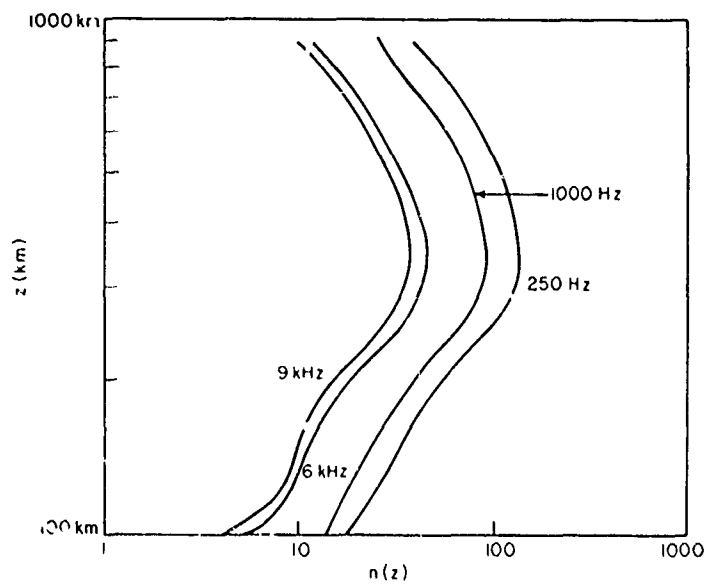


Fig. 11—Index of refraction vs height of the whistler wave at several frequencies

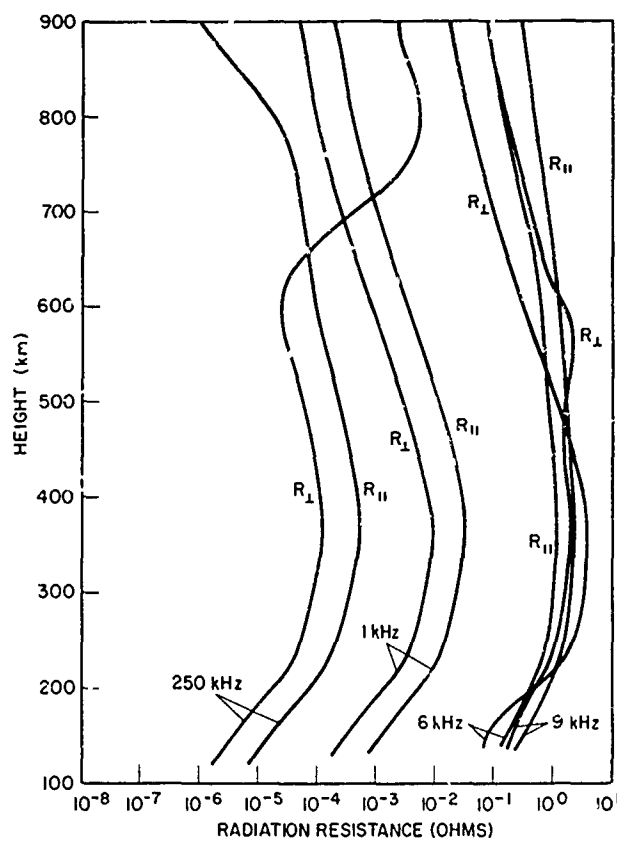


Fig. 12—Radiation resistances of a 100-m radius loop at several frequencies and heights in the ionosphere, and for loop dipole orientations parallel ( $R_{||}$ ) and perpendicular ( $R_{\perp}$ ) to the earth's magnetic field. Values of  $R_{\perp}$  were used in computing Tables 1 through 4.

NRL REPORT 8032

Table 1 — Compilation of Required Power Results for a  $10^4$ -kg, 100-m Radius Loop Transmitting Antenna for  $y = 1$  Mm\*

$f(\text{Hz})$	$z_s(\text{km})$	$P_{\text{rad}}(\text{kW})$	$P_{\text{ohmic}}(\text{kW})$	$P_{\text{total}}(\text{kW})$
250	120	$1.3 \times 10^1$	$1.9 \times 10^4$	$1.9 \times 10^4$
	300	$1.2 \times 10^2$	$3.6 \times 10^3$	$3.7 \times 10^3$
	800	$1.8 \times 10^4$	$9.4 \times 10^3$	$2.7 \times 10^4$
1000	120	$4.0 \times 10^0$	$1.3 \times 10^2$	$1.4 \times 10^2$
	300	$7.4 \times 10^1$	$2.7 \times 10^1$	$1.0 \times 10^2$
	800	$2.8 \times 10^0$	$7.3 \times 10^1$	$7.6 \times 10^1$
6000	120	$1.6 \times 10^0$	$8.6 \times 10^{-2}$	$1.7 \times 10^0$
	300	$1.8 \times 10^1$	$1.5 \times 10^{-2}$	$1.7 \times 10^1$
	800	$6.4 \times 10^{-1}$	$4.0 \times 10^{-2}$	$6.7 \times 10^{-1}$
9000	120	$4.5 \times 10^1$	$1.1 \times 10^0$	$4.7 \times 10^1$
	300	$1.5 \times 10^1$	$2.5 \times 10^{-1}$	$1.5 \times 10^1$
	800	$4.5 \times 10^1$	$6.8 \times 10^{-1}$	$4.5 \times 10^1$

\*Winter nighttime propagation and noise with  $S/N = 0$  dB in a 1-Hz bandwidth (Mediterranean Sea area).

Table 2 — Compilation of Required Power Results for a  $10^4$ -kg, 100-m Radius Loop Transmitting Antenna for  $y = 1$  Mm\*

$f(\text{Hz})$	$z_s(\text{km})$	$P_{\text{rad}}(\text{kW})$	$P_{\text{ohmic}}(\text{kW})$	$P_{\text{total}}(\text{kW})$
250	120	$5.2 \times 10^1$	$7.7 \times 10^4$	$7.7 \times 10^4$
	300	$4.7 \times 10^2$	$1.4 \times 10^4$	$1.5 \times 10^4$
	800	$7.2 \times 10^4$	$3.7 \times 10^4$	$1.1 \times 10^5$
1000	120	$5.0 \times 10^1$	$1.7 \times 10^3$	$1.7 \times 10^3$
	300	$9.3 \times 10^2$	$3.4 \times 10^2$	$1.3 \times 10^3$
	800	$3.5 \times 10^1$	$9.2 \times 10^2$	$9.5 \times 10^2$
6000	120	$2.6 \times 10^1$	$1.1 \times 10^0$	$2.7 \times 10^1$
	300	$2.8 \times 10^2$	$2.4 \times 10^{-1}$	$2.8 \times 10^2$
	800	$1.0 \times 10^1$	$6.6 \times 10^{-1}$	$1.1 \times 10^1$
9000	120	$1.8 \times 10^2$	$4.5 \times 10^0$	$1.8 \times 10^2$
	300	$6.0 \times 10^2$	$1.0 \times 10^1$	$6.0 \times 10^2$
	800	$1.8 \times 10^2$	$2.7 \times 10^0$	$1.8 \times 10^2$

\*Winter nighttime propagation and summer nighttime noise with  $S/N = 0$  dB in a 1-Hz bandwidth (Mediterranean Sea area).

KELLY, CHAYT AND BAKER

Table 3 — Compilation of Required Power Results for a  $10^4$ -kg, 100-m Radius Loop Transmitting Antenna for  $y = 1$  Mm\*

$f(\text{Hz})$	$z_s(\text{km})$	$P_{\text{rad}}(\text{kW})$	$P_{\text{ohmic}}(\text{kW})$	$P_{\text{total}}(\text{kW})$
250	120	$8.2 \times 10^2$	$1.2 \times 10^6$	$1.2 \times 10^8$
	300	$7.4 \times 10^3$	$2.3 \times 10^8$	$2.4 \times 10^8$
	800	$1.1 \times 10^8$	$5.9 \times 10^5$	$1.7 \times 10^8$
1000	120	$5.4 \times 10^4$	$1.8 \times 10^6$	$1.9 \times 10^6$
	300	$1.0 \times 10^8$	$3.7 \times 10^5$	$1.4 \times 10^8$
	800	$3.8 \times 10^4$	$9.9 \times 10^5$	$1.0 \times 10^8$
6000	120	$3.1 \times 10^4$	$1.3 \times 10^3$	$3.2 \times 10^4$
	300	$3.3 \times 10^5$	$2.8 \times 10^2$	$3.3 \times 10^5$
	800	$1.2 \times 10^4$	$7.8 \times 10^2$	$1.3 \times 10^4$
9000	120	$1.1 \times 10^5$	$3.0 \times 10^3$	$1.1 \times 10^5$
	300	$3.8 \times 10^5$	$6.5 \times 10^2$	$3.8 \times 10^5$
	800	$1.1 \times 10^5$	$1.7 \times 10^3$	$1.1 \times 10^5$

\*Daytime propagation and summer daytime with  $S/N = 0$  dB in a 1-Hz bandwidth (Mediterranean Sea area).

Table 4 — Compilation of Required Power Results for a  $10^4$ -kg, 100-m Radius Loop Transmitting Antenna for  $y = 1$  Mm\*

$f(\text{Hz})$	$z_s(\text{km})$	$P_{\text{rad}}(\text{kW})$	$P_{\text{ohmic}}(\text{kW})$	$P_{\text{total}}(\text{kW})$
250	120	$2.1 \times 10^2$	$3.1 \times 10^5$	$3.1 \times 10^5$
	300	$1.9 \times 10^3$	$5.7 \times 10^4$	$5.9 \times 10^4$
	800	$2.9 \times 10^5$	$1.5 \times 10^5$	$4.3 \times 10^5$
1000	120	$8.3 \times 10^2$	$2.8 \times 10^4$	$2.9 \times 10^4$
	300	$1.5 \times 10^4$	$5.7 \times 10^3$	$2.1 \times 10^4$
	800	$5.8 \times 10^2$	$1.5 \times 10^4$	$1.5 \times 10^4$
6000	120	$5.8 \times 10^2$	$2.6 \times 10^1$	$6.0 \times 10^2$
	300	$6.2 \times 10^3$	$5.4 \times 10^0$	$6.2 \times 10^3$
	800	$2.3 \times 10^2$	$1.5 \times 10^1$	$2.4 \times 10^2$
9000	120	$9.8 \times 10^3$	$2.5 \times 10^2$	$9.8 \times 10^3$
	300	$3.3 \times 10^4$	$5.5 \times 10^1$	$3.3 \times 10^4$
	800	$9.8 \times 10^3$	$1.4 \times 10^1$	$9.8 \times 10^3$

\*Daytime propagation and winter daytime noise with  $S/N = 0$  dB in a 1-Hz bandwidth (Mediterranean Sea area).

Table 5 — Nominal Ionospheric Transmission Losses Derived From the Calculations of [15] and [22-24]

$f(\text{Hz})$	Avg. Daytime Loss (dB)	Std. Deviation Daytime Models (dB)	Avg. Nighttime Loss (dB)	Std. Deviation Nighttime Models (dB)
250	9.8	3.2	1.6	0.1
1000	9.2	2.1	1.1	0.2
6000	16.8	3.9	1.6	0.7
9000	21.4	5.7	1.7	0.8

Table 6 — Nominal Daytime Attenuation Rates in the Earth-Ionosphere Cavity Based on Six Models Used by Barr [7]

$f(\text{Hz})$	Avg. Daytime Attenuated Rate (dB/Mm)	Std. Deviation Daytime Models (dB/Mm)
250	3.8	1.2
1000	16.2	6.1
6000	8.5	3.3
9000	4.3	0.5

## DISCUSSION

The cases analyzed in Tables 1-4 should not be considered as selected optimum configurations or frequencies. The calculations only illustrate the broad range of required transmitter powers that can be obtained for different communication link requirements.

For the cases studied here, the time during which the satellite and groundbased receiver are in contact with each other is relatively brief. Assuming that the ionospheric exit point is moving at a typical satellite velocity of 5 km/s, the maximum contact time while a 1000-km radius coverage area moves over a fixed receiver location would be approximately 7 min.

In the results shown in Tables 1-4, we have not optimized the transmitting loop antenna radius to the full extent possible. Further calculations indicate that at the 250-Hz frequency considered here, a more balanced distribution of input power between radiation and ohmic losses may be accomplished by increasing the loop antenna radius beyond the value of 100 m assumed for Table 1. This increase of radius (keeping the total mass fixed) tends to increase the ohmic resistance as the square of the loop radius. The loop radiation resistance (and the power injected into the earth-ionosphere waveguide) increases in proportion to the fourth power of the loop radius. For example, using a 1000-m radius loop, this type of extrapolation implies that under winter nighttime conditions, the total required power for a 250-Hz satellite transmitter at a 300-km altitude height is 614 kW with 470 kW radiated and 144 kW of ohmic losses using a  $10^4$ -kg antenna. A more exact calculation at 250 Hz leads to the total power requirement of 799 kW with 736 kW radiated and 63 kW of ohmic losses. Obviously, some provision must be made for radiating the heat generated by the ohmic losses of the antenna.



The results also indicate that the transmitter power required to produce a given S/N ratio at a given point on the earth's surface ranges from less than a kilowatt to thousands of megawatts, depending on the many variables affecting the signal and noise levels. If we limit ourselves to the results for a 6-kHz transmitter operating at 800 km, the power required to produce a 0-dB S/N ratio in a 1-Hz bandwidth varies from less than a kilowatt for winter nighttime conditions to several megawatts for summer daytime conditions. This large variation occurs because the noise varies by about 19 dB and the signal by about 13 dB. In addition, the poorest signal and highest noise occur during summer day, while the best signal and lowest noise occur during winter night.

One may conclude from this study that it is certainly possible to achieve some communications during the optimum period using relatively low-powered (few kilowatts) transmissions, but that, at the sample frequencies considered (250 Hz, 1 kHz, and 9 kHz), a truly effective system would require increasing powers up to the several-megawatt range and beyond, since greater data rate and coverage area are always desirable.

The U.S. National Aeronautics and Space Administration (NASA) and the Energy Research and Development Administration (ERDA) are studying plans and proposals for future space nuclear and solar electric power sources which range in power from a few kilowatts to thousands of megawatts [25-33]. The expected operation of the reusable NASA space shuttle would make the launch and deployment of a reasonably large power source and transmitting antenna feasible and possibly economical.

#### ACKNOWLEDGMENTS

We wish to thank B. Wald, W. Ament, W.E. Garner, and L.S. Bearce for their encouragement and advice. The research reported here was sponsored by the Office of Naval Research and National Aeronautics and Space Administration.

#### REFERENCES

1. J. Galejs, "Excitation of the Terrestrial Wave guide by Sources in the Lower Ionosphere," *Radio Sci.*, 6, 41-53 (Jan. 1971).
2. J. Galejs, "Stable Solution of Ionospheric Fields in the Propagation of ELF and VLF Waves," *Radio Sci.* 7, 549-561 May, (1972).
3. F. Einaudi and J.R. Wait, "Analysis of the Excitation of the Earth-Ionosphere Waveguide by a Satellite-Borne Antenna," *Can J. Phys.* 49, 449 (Feb. 1971).
4. F. Einaudi and J.R. Wait, "Analysis of the Excitation of the Earth-Ionosphere Waveguide by a Satellite-Borne Antenna II," *Can. J. Phys.* 49, 1452-1460 (June 1971).
5. R.A. Pappert, "Excitation of the Earth-Ionosphere Waveguide by Point Dipoles at Satellite Heights," *Radio Sci.* 8, 535-545 (June 1973).
6. D.J. Baker, G.A. Chayt, and F.J. Kelly, "Radiation from Loop Antennas Imbedded in a Magnetoplasma," NRL Report 8024 (to be published).
7. R. Esiri, "The Attenuation of ELF and VLF Radio Waves Propagating Below Inhomogeneous Isotropic Ionospheres," *J. Atmos. Terr. Phys.* 32, 1781-1791, (Nov. 1970).

NRL REPORT 8032

8. R. Barr, "The ELF and VLF Amplitude Spectrum of Atmospherics with Particular Reference to the Attenuation Band Near 3 kHz," *J. Atmos. Terr. Phys.* 32, 977 (June 1970).
9. R. Barr, "The Propagation of ELF and VLF Radio Waves Beneath an Inhomogeneous Anisotropic Ionosphere," *J. Atmos. Terr. Phys.* 33, 343 (Mar. 1971).
10. R. Barr, "The Effect of the Earth's Magnetic Field on the Propagation of ELF and VLF Radio Waves," *J. Atmos. Terr. Phys.* 33, 1577 (Oct. 1971).
11. R. Barr, "Some New Features of ELF Attenuation," *J. Atmos. Terr. Phys.*, 34, 411 (Mar. 1972).
12. J. Galejs, *Terrestrial Propagation of Long Electromagnetic Waves*, Pergamon Press, Oxford, 1972.
13. J.R. Wait, *Electromagnetic Waves in Stratified Media*, Pergamon Press, New York, 1962.
14. R.A. Pappert, W.F. Moler, and L.R. Shockey "A FORTRAN Program for Waveguide Propagation which Allows Both Vertical and Horizontal Dipole Excitation," Naval Electronics Laboratory Center Interim Report No. 702 for DASA, June 1970.
15. M.L.V. Pitteway and J.L. Jespersen, "A Numerical Study of the Excitation, Internal Reflection and Limiting Polarization of Whistler Waves in the Lower Ionosphere," *J. Atmos. Terr. Phys.* 28, 17 (Jan. 1966).
16. M.L.V. Pitteway, "The Numerical Calculation of Wave-Fields, Reflexion Coefficients and Polarizations for Long Radio Waves in the Lower Ionosphere. I," *Phil. Trans. R. Soc.* A257, 219 (Mar. 1965).
17. W.R. Piggott, M.L.V. Pitteway, and E.V. Thrane, "The Numerical Calculation of Wave Fields, Reflexion Coefficients and Polarizations for Long Radio Waves in the Lower Ionosphere. II," *Phil. Trans. R. Soc.*, A257, 243 (Mar. 1965).
18. V.L. Ginzburg, "Propagation of Electromagnetic Waves in Plasma," Gordon and Breach Science Publishers, Inc., New York, 1961.
19. F.J. Kelly, D.J. Baker and G.A. Chayt, "On the Spreading of Waves Launched by an ELF/VLF Satellite," NRL Report 7814, September 1974.
20. A.D. Watt, *V.L.F. Radio Engineering*, Pergamon Press, New York, 1967.
21. J.R. Davis, private communication.
22. H.G. Booker, C.M. Crain, and E.C. Field, Jr., "Transmission of Electromagnetic Waves Through Normal and Disturbed Ionospheres", Proc. of the Conf. on Antennas and Transionospheric Propagation as related to ELF/VLF Downlink Satellite Communications, NRL Report 7462, November 27, 1972.
23. Ya.L. Al'pert and D.S. Fligel, *Propagation of ELF and VLF Waves Near the Earth*, Consultants Bureau, New York-London, 1970.
24. R.A. Helliwell, *Whistlers and Related Ionospheric Phenomena*, Stanford U. Press, Stanford, California, 1965.
25. G.R. Woodcock and D.L. Gregory, "Economics Analyses of Solar Energy Utilization," 9th Intersociety Energy Conversion Engineering Conference Proceedings (ASME), 306-316 1974.

KELLY, CHAYT AND BAKER

26. P.E. Glaser, O.E. Maynard, J. Mackovciak, Jr. and E.L. Ralph, "Feasibility Study of a Satellite Solar Power Station," NASA CR-2357, February 1974.
27. J.T. Patha and G.R. Woodcock, "Feasibility of Large Scale Orbital Solar/Thermal Power Generation," 8th Intersociety Energy Conversion Engineering Conference Proceedings, (AIAA), 312-319 August 1973.
28. J.R. Williams and J.D. Clement, "The Satellite Nuclear Power Station, An Option for Future Power Generation," 8th Intersociety Energy Conversion Engineering Conference Proceedings (AIAA), 566-573 August 1973.
29. Y.S. Tang, J.S. Stefanko, P.W. Dickson and D.W. Drawbaugh, "An Engineering Study of the Colloid-Fueled Reactor Concept," *J. Spacecraft and Rockets* 8 (2), 129-133 (Feb. 1971).
30. J.H. Pitts and C.E. Walter, "Conceptual Design of a 10-Mw<sub>e</sub> Nuclear Rankine System for Space Power," *J. Spacecraft and Rockets* 7 (3), (Mar. 1970).
31. L.H. Boman and J.G. Gallagher, "NERVA Technology Reactor Integrated with NASA Lewis Brayton Cycle Space Power Systems," *J. Spacecraft and Rockets* 8 (5), 500-505 (May 1971).
32. J.H. Pitts and C.E. Walter, "Conceptual Design of a 2-Mw<sub>e</sub> (375 kw<sub>e</sub>) Nuclear-Electric Space Power System," *J. Spacecraft and Rockets* 7 1282-1286 (Nov. 1970).
33. G.R. Seikel and L.D. Nichols, "Potential of Nuclear MHD Electric Power Systems," *J. Spacecraft and Rockets* 9 (5), 322-326 (May 1972).